

Preliminary Assessment on Thermal Hydraulic Performance of Molten Salt and Metal Reactor (MSMR) by using FLUENT code

Won Jun Choi^a, Juhyeong Lee^a, Yonghee Kim^c and Sung Joong Kim^{*a,b}

^aDepartment of Nuclear Engineering, Hanyang University
222 Wangsimni-ro, Seongdong-gu, Seoul 04763, Republic of Korea

^bInstitute of Nano Science and Technology, Hanyang University
222 Wangsimni-ro, Seongdong-gu, Seoul 04763, Republic of Korea

^cDepartment of Nuclear and Quantum Engineering, Korea Advanced Institute of Science and Technology
291 Daehak-ro, Yuseong-gu, Daejeon 34141, Republic of Korea

* Corresponding author: sungjkim@hanyang.ac.kr

***Keywords :** molten salt and metal reactor, computational fluid dynamics code, assessment of thermal output

1. Introduction

Nuclear power generation is being utilized actively due to attractive characteristics such as a low sensitivity from climate change and achievement of carbon-neutral. The commercial reactor has been designed as a large size for taking economic advantages. Consequently, the commercial reactor is required to be installed nearby less populated ocean for the procurement of coolant and minimization of human casualty.

Recently, the research on the miniaturization of nuclear reactors is being performed to overcome the geographical constraints. The Korea Advanced Institute of Science and Technology (KAIST) proposed a new type of micro reactor called as molten salt and metal reactor (MSMR) [1]. MSMR was designed for the accomplishment of specific purposes such as a spacecraft propulsion and electricity supply to the remote area. Figure 1 shows a schematic of MSMR.

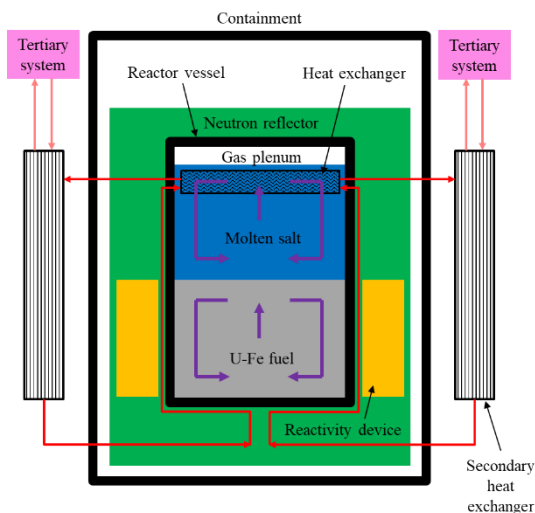


Figure 1. Schematic of molten salt and metal reactor (MSMR)

The reactor vessel of MSMR includes two liquid layers as shown in Fig. 1. The liquid metal fuel and molten coolant salt exist at the lower region and upper region of the reactor vessel, respectively. The decay heat generated due to the nuclear fission of the liquid metal

fuel is transferred to the molten coolant salt located at the upper region through the liquid-liquid interface. Simultaneously, the decay heat is transferred to the secondary molten coolant salt flowing along the outer wall of reactor vessel. The transferred heat through the liquid-liquid interface and secondary molten coolant salt is exchanged through the primary heat exchanger located at the upper part of the reactor vessel. The heat transferred to the primary heat exchanger is removed through the secondary heat exchanger located at the outside of containment as shown in Fig. 1. The heat in the secondary heat exchanger is consequently removed through the tertiary system.

The feasibility on the aforementioned heat transfer mechanism of MSMR is required to be assessed. Thus, in this study, the numerical calculation was performed for the investigation of thermal hydraulic performance on MSMR by using the FLUENT code.

2. Numerical methodology

2.1. Geometry

The geometry on the analysis domain was fabricated through SpaceClaim 2022 R1 as a one of computer-aided design (CAD) software. SpaceClaim has been utilized frequently owing to several advantages such as the simplification of CAD data and easily coupling with computational fluid dynamics (CFD) software. Figure 2 shows the geometry of MSMR made by CAD software. The analysis geometry was designed as a cylinder shape for the simulation of cylindrical reactor vessel. The cylindrical geometry was partitioned as two parts: fuel cell zone and coolant cell zone.

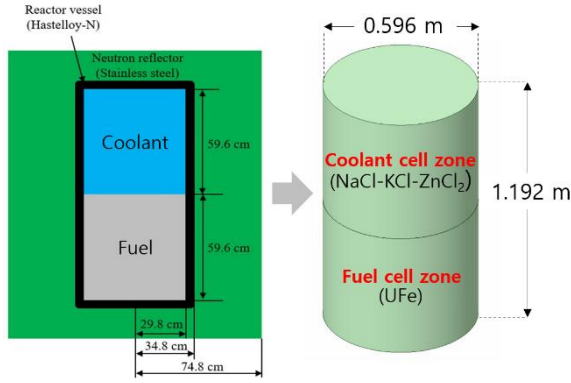


Figure 2. Geometry of reactor vessel fabricated through CAD software

2.2. Numerical analysis conditions

The numerical calculation was performed to investigate the thermal hydraulic performance of MSMR by using FLUENT 2022 R1 code, which is a one of CFD codes. The fuel (UFe) and coolant materials (NaCl-KCl-ZnCl₂) were assigned at the fuel and coolant cell zones, respectively. The material properties of liquid metal fuel and molten coolant salt are presented in Table 1. All material properties except density where the Boussinesq approximation was applied were assumed as constant values for simplification of calculation. The natural convection was simulated according to density differences based on the Boussinesq approximation.

Table 1. Material properties of liquid metal fuel and molten coolant salt

Material Properties	UFe	NaCl-KCl-ZnCl ₂
Specific heat [J/kg K]	512.67	900
Molar mass [g/mol]	349.38	73.89
Density [kg/m ³]	13200	2787
Viscosity [Pa s]	0.0056	0.00446
Thermal conductivity [W/m K]	10	0.35
Thermal expansion coefficient [K ⁻¹]	3.875×10 ⁻⁵	32.663×10 ⁻⁵

The iterative solver was selected as a pressure-based model for the stable calculation. The volume of fluid (VOF) method was used as a multiphase model for the interface tracking [2]. Radiation heat transfer model was not reflected in this calculation for the conservative approach. The other numerical analysis conditions are presented in Table 2.

Table 2. Numerical analysis conditions

Parameters	Values
Solver	1) Pressure-based solver 2) Transient calculation
Phase model	Multiphase model (VOF)
Viscous model	Laminar

Radiation model	-
Interface condition	Matching option
Time step	0.001~0.007 (Global courant number ~1)
Pressure-velocity coupling	Coupled method
Transient formulation	First order implicit

2.3. Test matrix

The test matrix was constructed based on the analytic results calculated through the discretization of Eq. (1), which is a cylindrical coordinate (r, z) conduction equation [3]. Equation (1) includes r, z, k, T, q''' , ρ, t and c_p which are radial length, axial length, thermal conductivity, temperature, volumetric heat generation, density, time and specific heat at constant pressure, respectively.

$$\frac{1}{r} \frac{\partial}{\partial r} \left(rk \frac{\partial T}{\partial r} \right) + \frac{\partial}{\partial z} \left(k \frac{\partial T}{\partial z} \right) + q''' = \rho c_p \frac{\partial T}{\partial t} \quad (1)$$

The analytic solutions which solely considered the conduction among nodes were derived as 300~600 kW. Conversely, the numerical simulation through the FLUENT code included the convection as well as the conduction. It was predicted that the available thermal output calculated through FLUENT code might be higher than analytic solutions. Accordingly, a minimum value of thermal output in the test matrix was selected as 600 kW, which is a maximum value of analytic solutions. The thermal output interval in a test matrix was established as 200 kW to consider the wider range. Consequently, the thermal output range in a test matrix was set as 600~1000 kW.

The wall temperature was selected as 600 K and 700 K by considering the melting temperature of molten coolant salt (500 K) at the upper region [4]. Table 3 shows the test matrix for the numerical calculation. Based on the values at the test matrix, the available thermal output was investigated according to the modification of thermal output and wall temperature as shown in Fig. 3. The thermal output was simulated through the application of uniform heat source in the fuel cell zone.

Table 3. Test matrix for the numerical calculation

Case	Thermal output (Q) [kW]	Wall temperature (T) [K]
01	600	600
02	800	600
03	1000	600
04	600	700
05	800	700
06	1000	700

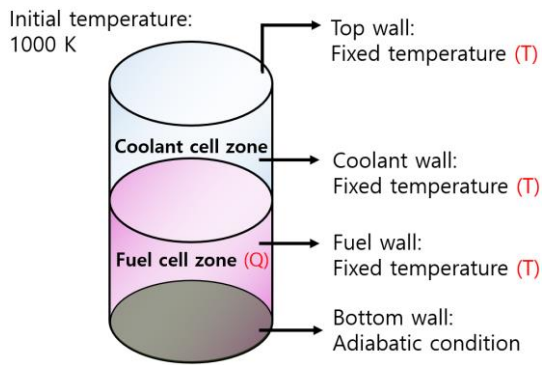


Figure 3. Initial and boundary conditions

The proper criteria were established for the assessment of available thermal output. It was regarded as the acceptable case when the net heat, which is a summation of heat generation and heat removal, becomes negative values or converges to zero. The case where the peak temperature exceeded 1300 K was regarded as the unacceptable case for the secure of material integrity.

3. Results and discussion

Table 4 shows the criterion time taken to reach the aforementioned criteria in the simulation. Table 5 shows the amount of net heat and heat transfer through the boundary walls at the criterion time. Table 6 shows the peak and average temperature at the criterion time.

Table 4. Criterion time taken to reach the established criteria

Case	01	02	03	04	05	06
Time [s]	708	714	5511	755	5007	1726

Table 5. Amount of heat transfer through the boundary wall and net heat at the criterion time

Case	Fuel wall [kW]	Coolant wall [kW]	Top wall [kW]	Net [kW]
01	-613.07	-26.23	-5.41	-44.9
02	-765.08	-28.87	-5.81	-0.018
03	-957.84	-33	-6.61	2.22
04	-574.22	-21.32	-4.29	-0.02
05	-766.23	-26.28	-5.22	2.02
06	-928.31	-27.70	-5.42	38.25

Table 6. Peak temperature and volumetric average temperature at the criterion time

Case	Peak temperature [K]		Average temperature [K]	
	Fuel	Coolant	Fuel	Coolant
01	1042.6	1032.3	940.5	972.6
02	1118.2	1091.7	1010.6	988.8
03	1230.2	1200.1	1113.4	1042.3
04	1094.6	1068.6	1009.6	988.1
05	1209.8	1176.8	1111.3	1050.3
06	1300.1	1238.9	1197.7	1062.9

According to the criteria and calculation results, case 01, 02 and 04 were assessed as acceptable cases based on

the negative net heat. Figures 4 and 5 show the change of net heat and temperature on the case 01, 02 and 04, respectively. The generated heat from the heat source in the fuel cell zone was removed dominantly from the fuel wall as shown in Table 5. On the other side, the heat transfer across the liquid-liquid interface exhibited low efficiency due to a small heat transfer area of interface as 0.28 m². Accordingly, at the case 01, the fuel temperature was lower than the coolant temperature due to the comparatively small thermal output and large amount of heat transfer through the fuel wall as shown in Figure 5.

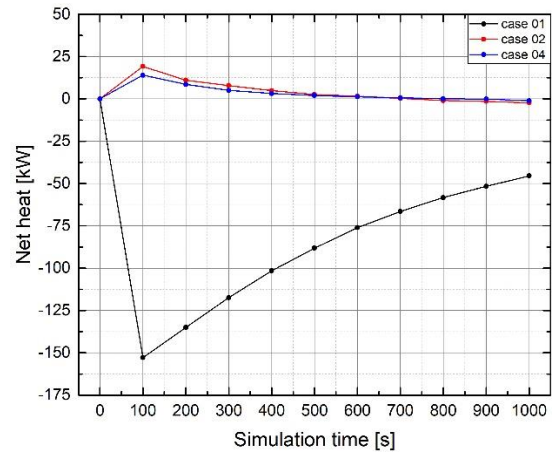


Figure 4. Net heat change of case 01, 02 and 04

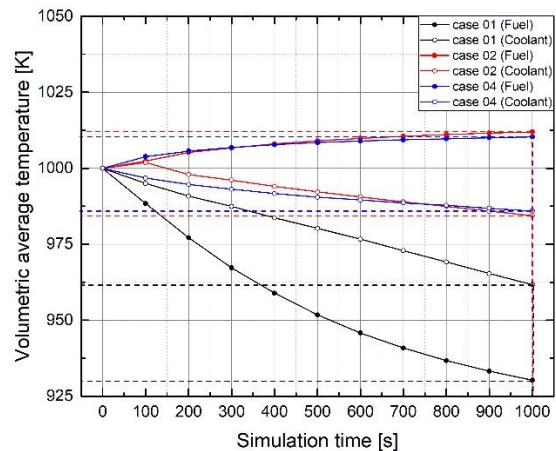


Figure 5. Volumetric average temperature change of case 01, 02 and 04

Case 03 and 05 were also evaluated as acceptable cases according to the convergence of net heat into zero. The temperature variations became slight as the net heat got close to the zero. Figures 6 and 7 show the change of net heat and temperature on the case 03 and 05. On the other hand, the peak temperature in the case 06 reaches 1300 K at the 1726 seconds as shown in Tables 4 and 6. Case 06 was assessed as the unacceptable case based on the criterion. It means that the 1000 kW thermal output at the wall temperature of 700 K is not allowable. In conclusion, the available thermal output of MSMR was assessed as 1000 kW and 800 kW at the 600 K and 700 K of the wall temperature, respectively.

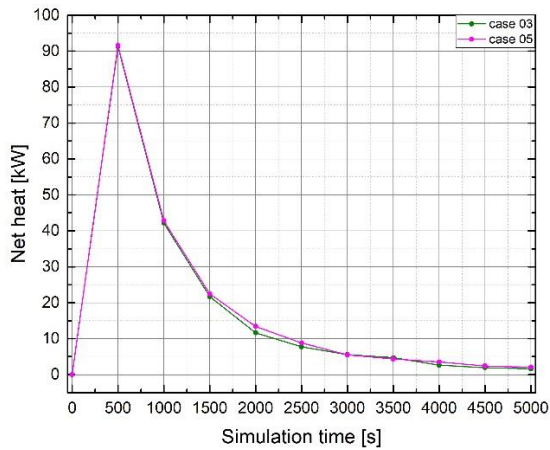


Figure 6. Net heat change of case 03 and 05

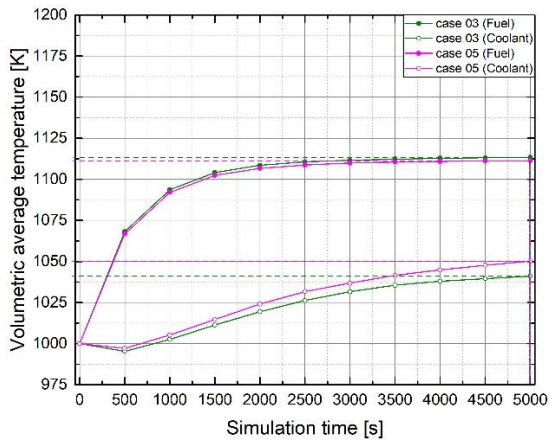


Figure 7. Volumetric average temperature change of case 03 and 05

Table 7 shows the volumetric averaged velocity at the criterion time. The heat is uniformly generated over the whole region of fuel cell zone. The uniform heat generation over the entire fuel region induces the directionless and irregular flow of fuel. On the other hand, the coolant receives the generated heat from the fuel region located at the lower part. Simultaneously, the heat is removed through top and coolant walls. The relatively regular natural convection is induced at the coolant region since the upward and downward flow occur at the center and side of coolant region, respectively. Thus, the volumetric averaged velocity at the coolant region was faster than the fuel region. Figure 8 shows the velocity and temperature contour of the case 02.

Table 7. Volumetric averaged velocity at the criterion time

Case	Fuel velocity [m/s]	Coolant velocity [m/s]
01	0.0074	0.016
02	0.0082	0.021
03	0.0086	0.031
04	0.0074	0.019
05	0.0078	0.026
06	0.0088	0.032

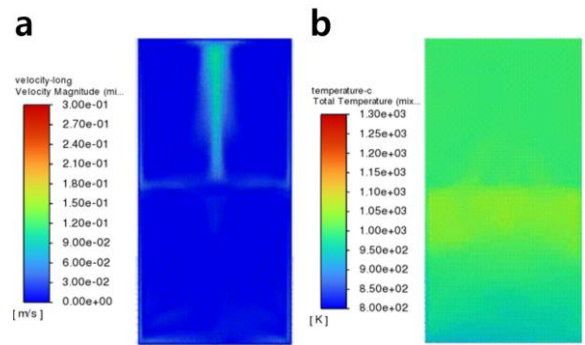


Figure 8. (a) Velocity and (b) temperature contour in the case 02

4. Conclusion

This study aimed to investigate the thermal hydraulic performance of MSMR by using FLUENT code. The major findings of this study can be summarized as follows:

- ✓ Allowable thermal output of MSMR was assessed as 1000 kW and 800 kW under the wall temperature of 600 K and 700 K, respectively.
- ✓ The generated heat from the heat source was removed dominantly from the fuel wall.
- ✓ The heat transfer across the liquid-liquid interface exhibited low efficiency.
- ✓ The velocity of coolant region was faster than the velocity of fuel region due to relatively regular natural convection.

The further study including radiation heat transfer model and heat exchanger model is required to be performed for the accurate analysis. In addition, the design of additional facilities such as a heat pipe to facilitate the heat transfer across the interface is needed.

Acknowledgments

This research was supported by the National Research Foundation of Korea (NRF) and funded by the ministry of Science, ICT, and Future Planning, Republic of Korea (grant numbers NRF-2021M2D2A2076382).

REFERENCES

- [1] Lee, Eunhyug, et al. "LEU-based Molten Salt and Metal Reactor for Ultramicro Miniaturization."
- [2] Hirt, Cyril W., and Billy D. Nichols. "Volume of fluid (VOF) method for the dynamics of free boundaries." *Journal of computational physics* 39.1 (1981): 201-225.
- [3] Tsega, Endalew Getnet. "Numerical solution of three-dimensional transient heat conduction equation in cylindrical coordinates." *Journal of Applied Mathematics* 2022 (2022): 1-8.
- [4] Lan, Zhi-An, et al. "Ionothermal Synthesis of Covalent Triazine Frameworks in a NaCl-KCl-ZnCl₂ Eutectic Salt for the Hydrogen Evolution Reaction." *Angewandte Chemie International Edition* 61.18 (2022): e202201482.